

Causal Deconfounding via Confounder Disentanglement for Dual-Target Cross-Domain Recommendation

Jiajie Zhu, Yan Wang*, Senior Member, IEEE, Feng Zhu and Zhu Sun

Abstract—In recent years, dual-target Cross-Domain Recommendation (CDR) has been proposed to capture comprehensive user preferences in order to ultimately enhance the recommendation accuracy in both data-richer and data-sparser domains simultaneously. However, in addition to users’ true preferences, the user-item interactions might also be affected by confounders (e.g., free shipping, sales promotion). As a result, dual-target CDR has to meet two challenges: (1) how to effectively decouple observed confounders, including single-domain confounders and cross-domain confounders, and (2) how to preserve the positive effects of observed confounders on predicted interactions, while eliminating their negative effects on capturing comprehensive user preferences. To address the above two challenges, we propose a Causal Deconfounding framework via Confounder Disentanglement for dual-target Cross-Domain Recommendation, called CD2CDR. In CD2CDR, we first propose a confounder disentanglement module to effectively decouple observed single-domain and cross-domain confounders. We then propose a causal deconfounding module to preserve the positive effects of such observed confounders and eliminate their negative effects via backdoor adjustment, thereby enhancing the recommendation accuracy in each domain. Extensive experiments conducted on five real-world datasets demonstrate that CD2CDR significantly outperforms the state-of-the-art methods.

Index Terms—Cross-Domain Recommendation, Confounder Disentanglement, Causal Deconfounding.

I. INTRODUCTION

DUAL-TARGET Cross-Domain Recommendation (CDR) [1] aims to capture comprehensive user preferences, and thus enhance the recommendation accuracy in both data-richer and data-sparser domains simultaneously, which are source domains and target domains as well. However, in addition to users’ true preferences, the user-item interactions might also be affected by confounding factors. A confounding factor, termed as *confounder* in causal inference [2], [3], affects both the treatment and the outcome [4], [5], which can be broadly interpreted as user preference and user-item interaction respectively (see Fig. 1(a)) in the context of recommender systems (RSs) [6], [7].

*Yan Wang is the corresponding author.

Jiajie Zhu and Yan Wang are with the School of Computing, Macquarie University, Sydney NSW 2109, Australia (E-mail: jiajie.zhu1@students.mq.edu.au, yan.wang@mq.edu.au).

Feng Zhu is with the Ant Group, Hangzhou, China (E-mail: zhufeng.zhu@antgroup.com).

Zhu Sun is with the Centre of Frontier AI Research, Institute of High Performance Computing, Agency for Science, Technology and Research, Singapore (E-mail: sunzhuntu@gmail.com).

In the dual-target CDR scenario, the observed confounders can be categorized into two types, i.e., *single-domain confounder* (SDC) and *cross-domain confounder* (CDC). SDC only affects user preference and user-item interaction in one specific domain and has been widely studied in the existing literature [8], [9]. By contrast, CDC affects both domains; however, it has been overlooked in existing dual-target CDR methods. Because SDC is essentially a simplified version of CDC, below we particularly introduce our in-depth analysis of CDCs with examples in e-commerce platforms, such as Tmall and Amazon, where ‘purchase’ and ‘add to favorite’ activities of users are considered as two domains in line with the existing works [10], [11].

Cross-domain confounders have both positive and negative impacts on predicting user-item interactions in both domains. For example, as illustrated in Fig. 1(b), ‘sales promotion’ is a CDC, because it simultaneously affects both ‘purchase’ and ‘add to favorite’ domains. On the one hand, this ‘sales promotion’ CDC has a positive impact. In fact, while Alice’s true preference is the primary cause of her behaviors in both domains, ‘sales promotion’ is a secondary cause that serves as a catalyst. With a new sales promotion on dresses #1 and #2, both of which Alice likes but previously found over her budget, she immediately purchases dress #1 that has become affordable within her budget. By contrast, since the discounted price of dress #2 is still over her budget, she adds it to favorite for future consideration, looking forward to a further price reduction. On the other hand, this ‘sales promotion’ CDC has a negative impact too. As depicted in Fig. 1(c), a data-driven RS improperly perceives ‘sales promotion’ (i.e., a CDC) as Alice’s preference in both domains. As a result, the data-driven RS mistakenly recommends dresses #3 and #4 with sales promotion to Alice, but Alice actually does not like them. This misalignment, referred to as *confounding bias* [12], results in biased recommendations. Similarly, SDCs (e.g., ‘free shipping’ shown in Figs. 1(d)-1(e)) also have both positive and negative impacts on predicting user-item interactions in their respective domains.

Based on the above discussion, an effective dual-target CDR should *deconfound both observed single-domain and cross-domain confounders*, which includes three tasks, namely, (1) identify and decouple such observed confounders, (2) preserve their positive impacts on predicted interactions, and (3) eliminate their negative impacts on user preferences [13]. However, existing dual-target CDR approaches overlook the above observations. Thus, a novel dual-target CDR model

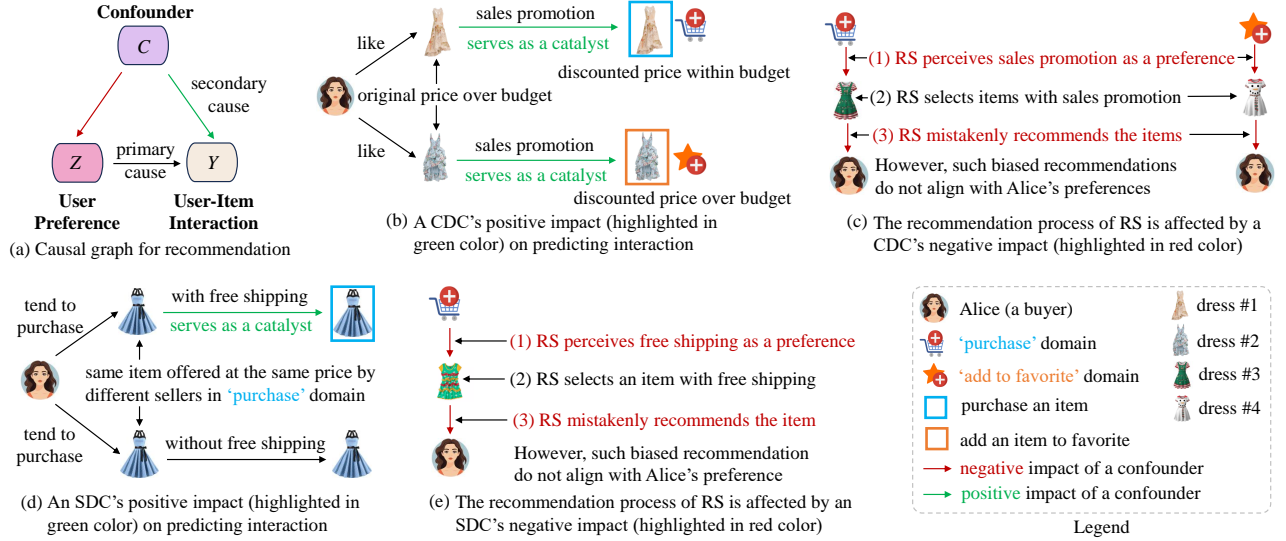


Fig. 1. Examples to depict single-domain confounder (SDC) and cross-domain confounder (CDC) in a dual-target CDR [14].

should be proposed to incorporate such insights for comprehensively understanding user-item interactions.

To effectively advance dual-target CDR, the following two key challenges need to be addressed.

CH1. *How to effectively decouple observed cross-domain confounders in addition to single-domain confounders to comprehensively understand user-item interactions in dual-target CDR?* The existing dual-target CDR methods either employ graph clustering strategy [15] and variational information bottleneck [16], or identify unobserved domain-specific confounders first, and then utilize causal techniques, e.g., inverse propensity score (IPS) estimators [10] and invariant learning [11], to obtain debiased representations (it is worth mentioning that domain-specific confounders in existing works are different from SDCs in our work, see Section II-B for elaboration). However, none of them explicitly decouples observed cross-domain confounders, and thus it is hard to obtain a comprehensive understanding of user-item interactions in each of both domains.

CH2. *How to preserve the positive impacts of observed confounders on predicted interactions, while eliminating their negative impacts on capturing comprehensive user preferences, thereby enhancing the recommendation accuracy in both domains?* Most existing causal methods [17], [18] tend to eliminate the confounders' negative impacts, in order to obtain the debiased comprehensive user preferences for recommendation. However, most of them overlook the confounders' positive impacts, and thus limit their efficacy in enhancing the recommendation accuracy [19].

Our Approach and Contributions. To address the above two challenges, we propose a novel causal deconfounding framework via confounder disentanglement for dual-target CDR. To the best of our knowledge, this is the first work in the literature that explicitly decouples observed cross-domain confounders, and incorporates observed confounders' positive impacts into debiased comprehensive user preferences for dual-target CDR. The characteristics and contributions of our framework can be summarized as follows:

- We first propose a **Causal Deconfounding** framework

via **Confounder Disentanglement** for dual-target **Cross-Domain Recommendation**, called **CD2CDR**, which can disentangle two types of observed confounders, eliminate their negative impacts to obtain debiased preferences, and preserve such confounders' positive impacts, thereby enhancing the recommendation accuracy in both domains;

- To address **CH1**, we propose a confounder disentanglement module to effectively disentangle observed SDCs and CDCs. In this module, we devise a dual adversarial structure to disentangle SDCs in each domain and applies half-sibling regression to decouple CDCs, thus obtaining a comprehensive understanding of user-item interactions in each of both domains;
- To address **CH2**, we propose a causal deconfounding module to deconfound disentangled observed SDCs and CDCs via backdoor adjustment. Specifically, we design a confounder selection function to mitigate such observed confounders' negative effects, thereby recovering debiased comprehensive user preferences. We then incorporate the observed confounders' positive effects into such debiased preferences to enhance the recommendation accuracy in both domains;
- Extensive experiments conducted on five real-world datasets show that our CD2CDR outperforms the best-performing state-of-the-art baseline with an average increase of 6.64% and 8.92% w.r.t. HR@10 and NDCG@10, respectively.

II. RELATED WORK

A. Single-Target and Dual-Target CDR

Single-Target CDR. Single-Target CDR [20] focuses on addressing the data sparsity problem by utilizing the abundant information available in a data-richer domain to improve the recommendation performance in a data-sparser domain. The existing single-target CDR approaches can be divided into two categories: (1) content-based transfer, and (2) feature-based transfer [20]. Content-based transfer [21] leverages user/item attributes and textual information to establish links across domains. By contrast, feature-based transfer [22], [23] employs

machine learning techniques to extract user/item embeddings or rating patterns [24] for cross-domain transfer.

Dual-Target CDR. Unlike single-target CDR, dual-target CDR [1] aims to enhance the recommendation accuracy in both data-richer and data-sparser domains by bidirectionally sharing knowledge, providing a basis for its expansion into Multi-Target CDR [25], [26]. The existing dual-target CDR methods can be roughly classified into two classes: (1) conventional methods, and (2) disentanglement-based methods. Conventional methods utilize two base encoders to transform each domain's interaction data into embeddings, which are then symmetrically incorporated through various transfer layers [27], [28]. By contrast, disentanglement-based methods employ variational autoencoder (VAE) [29] or other decoupling approaches [30] to disentangle domain-shared user preferences for common knowledge transfer, and then incorporate such information with decoupled domain-specific or domain-independent user preferences to capture comprehensive user preferences. However, these methods overlook that, in addition to users' true preferences, users' final decisions are also influenced by confounders, which limits their ability to accurately predict user-item interactions, leading to suboptimal recommendation results.

B. Deconfounded Recommendation

In recent years, causal learning [31], [32] has been introduced into RSs due to its ability to effectively tackle confounding problems arising from confounders, which can be classified into two types: observed confounders and unobserved confounders. For observed confounders, the existing deconfounded RSs adopt inverse propensity weighting (IPW) [33] or backdoor adjustment [9] to address the observed specific confounders, such as item popularity [8] and video duration [19]. For unobserved confounders, the existing deconfounded RSs either add additional assumptions [34], [35] or infer substitutes for confounders [36], [37] to alleviate the confounding bias.

Moreover, recent research efforts have extended confounder debiasing into cross-domain recommendation scenarios, focusing mainly on unobserved confounders. The unobserved confounders can be further categorized into two classes: domain-specific confounders (e.g., purchase-guided domain setting) and general confounders (e.g., the display position of items) [10]. Both classes cannot be captured from the datasets, and thus they are different from the observed SDCs and CDCs. Most of existing approaches tend to remove the negative influences of domain-specific confounders [10], [11] or general confounders [38], [39], but overlook the positive influences of such confounders, leading to an incomplete understanding of user-item interactions. In contrast to unobserved confounders, which are hidden and often difficult to estimate, observed confounders can be explicitly decoupled. As long as observed confounders are accurately disentangled, they can facilitate the design of effective deconfounding module for more precise deconfounding. However, none of existing approaches explicitly decouples observed cross-domain confounders, and preserves positive influences of confounders on user-item interactions,

and thus it is hard to achieve a comprehensive understanding of user-item interactions.

C. Disentangled Recommendation

Disentangled representation learning has recently gained increasing interest in RSs, aiming to decouple users' true preferences from confounding factors for more robust recommendation. For example, MacridVAE [40] models disentangled embeddings of user intentions from user-item interactions at both macro- and micro-level to reduce the impact of confounding factors. Moreover, DICE [41] tends to decouple users' interests and conformity to extract the desired causes of user-item interactions for robust recommendation. For causal recommendation, existing disentanglement-based methods [42] first decouple the semantic-aware intent embeddings, and then employ causal intervention [13] to alleviate the confounding bias. Unlike prior works, our work focuses on disentangling both observed single-domain and cross-domain confounders.

D. Deconfounded Domain Generalization

Domain generalization [43], [44] aims to train models on labeled data from source domains to enhance their generalization ability across unseen target domains by learning domain-invariant feature representations. However, the presence of confounders that affect both features and labels can compromise the validity of such representations, leading to models that fail to capture the true causal effects on the outcome. In recent years, causal inference techniques [45], [46] have been employed to address these confounding problems in domain generalization, thereby enhancing the model's ability to generalize accurately across varied domains. For instance, a line of existing works [47], [48] simply adopts the average value of all domain features in each domain as the confounder, and employs backdoor adjustment to capture the true causality. Another line of works incorporates interventional pseudo-correlation augmentation [49] or adversarial training [50] to remove the confounders to better generalize to the unseen domain. There is also another line of work that exploits the instrumental variables [51] or learns substitutes [52] to eliminate the unobserved confounders and capture the invariant features for domain generalization. However, most of the existing works either neglect domain-variant features or utilize off-the-shelf features as confounders instead of explicitly decoupling such confounders, which may result in downgrade deconfounding performance.

III. PRELIMINARIES

A. Problem Definition

For improved readability, we present the important notations used in this paper in Table I. The paper explores a fully overlapping dual-target CDR scenario in the domains D^A and D^B , with a common user set \mathcal{U} , the size of which is denoted as $m = |\mathcal{U}|$. Let \mathcal{V}^A (of size $n^A = |\mathcal{V}^A|$) and \mathcal{V}^B (of size $n^B = |\mathcal{V}^B|$) denote the item sets in the domains D^A and D^B , respectively. The raw feature vector of each item in D^A (or D^B) is defined as $\mathbf{E}_{vr}^A \in \mathbb{R}^{d^A}$ (or $\mathbf{E}_{vr}^B \in \mathbb{R}^{d^B}$), where d^A (or

TABLE I
IMPORTANT NOTATIONS.

Symbol	Definition
d	the embedding dimension
m	the number of users
n	the number of items
\mathcal{U}	the set of users
\mathcal{V}	the set of items
$\mathbf{R} \in \{0, 1\}^{m \times n}$	the rating matrix
y_{ij}	the interaction of user u_i on item v_j
$\hat{y}_{ij}, \hat{y}_{ik}$	the predicted user-item interactions
$*^A, *^B$	the notation for domain A and B , respectively
\mathbf{Z}_{sha}	the domain-shared user preferences
\mathbf{Z}_{spe}	the domain-specific user preferences
\mathbf{Z}_{ind}	the domain-independent user preferences
\mathbf{E}_u^*	the comprehensive user preferences
\mathbf{E}_v	the item embeddings
\mathbf{C}_{sd}	the single-domain confounders
\mathbf{C}_{cd}	the cross-domain confounders
$S(\cdot), T(\cdot)$	the generator in domain A and B , respectively
$H(\cdot)$	the discriminator
J	the number of cluster centroids
$p(c)$	the uniform distribution for prior probability
λ	the weight of cycle consistency loss
α	the regularization parameter
\mathbf{W}	the weight matrix

d^B) is the dimensionality of features. The interaction matrices are denoted as $\mathbf{R}^A \in \{0, 1\}^{m \times n^A}$ and $\mathbf{R}^B \in \{0, 1\}^{m \times n^B}$ in D^A and D^B , respectively.

To improve the performance of dual-target CDR, it is crucial to explicitly consider the impacts of observed confounders. These confounders include single-domain confounders \mathbf{C}_{sd} and cross-domain confounders \mathbf{C}_{cd} , both of which simultaneously influence user preferences and user-item interactions. Addressing the impacts of these confounders necessitates significant adjustments to existing dual-target CDR models. Hence, it is beneficial to propose a novel deconfounding framework that is highly extendable and compatible with most off-the-shelf dual-target CDR models. For this purpose, because DIDA-CDR [53] is a representative and state-of-the-art dual-target CDR model, we choose it as the foundation for our problem definition.

DIDA-CDR has effectively decoupled three essential components of user preferences for modeling comprehensive user preferences \mathbf{E}_u^* , thus achieving promising recommendation results in each domain. These three components include:

- (1) *domain-shared user preferences* \mathbf{Z}_{sha} , which have the same meaning in each of both domains. For instance, users might prefer items in the sports ‘category’, which is the domain-shared preference covering both the ‘purchase’ and ‘add to favorite’ domains, reflecting consistent preferences across these domains.
- (2) *domain-specific user preferences* \mathbf{Z}_{spe} , which are unique to one domain. For example, in the ‘add to favorite’ domain, users might prefer ‘luxurious’ items that they cannot afford to purchase but still wish to add them to favorite, while in the ‘purchase’ domain, users might prefer ‘practical’ items that offer good value for money.
- (3) *domain-independent user preferences* \mathbf{Z}_{ind} , which are seemingly common in both domains but have different meanings in each domain [53]. For instance, in the ‘purchase’ domain, ‘innovation’ refers to new functionalities in items

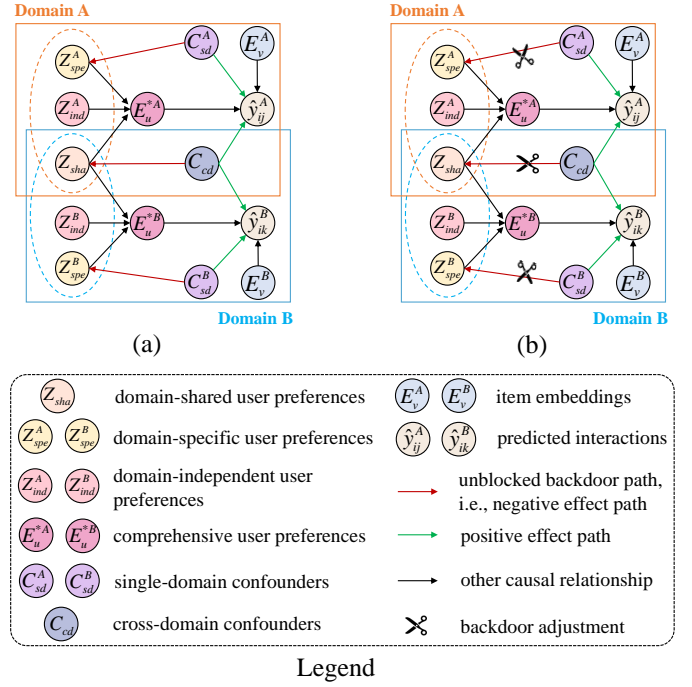


Fig. 2. Causal graphs of dual-target CDR for deconfounding observed SDCs and CDCs. (a) Original causal graph. (b) Deconfounded causal graph after eliminating such observed confounders’ negative effects by blocking backdoor paths via backdoor adjustment, as indicated by scissors [42].

that meet user needs, such as advanced functions in electronic devices that enhance user experience. In the ‘add to favorite’ domain, ‘innovation’ refers to avant-garde designs or conceptual items, like a chair with only armrests and legs but no seat. Such items, which are unique in design but low in practicality, are more likely to be added to favorite rather than purchased for actual use. Unlike domain-specific user preferences that only exist in their respective domain, domain-independent user preferences exist in both domains but take on different meanings in each domain.

Based on the above notations, the problem of Causal Deconfounding for Dual-Target CDR is defined as follows.

Causal Deconfounding for Dual-Target CDR. *Given the domain-specific and comprehensive user preferences (i.e., \mathbf{Z}_{spe} and \mathbf{E}_u^*) in each domain, the goal of causal deconfounding for dual-target CDR is to decouple observed single-domain confounders \mathbf{C}_{sd} and cross-domain confounders \mathbf{C}_{cd} , eliminate such observed confounders’ negative effects to obtain debiased comprehensive user preferences, and incorporate these confounders’ positive effects into such debiased preferences to get a comprehensive understanding of user-item interactions, thus enhancing the recommendation accuracy in both domains.*

B. Causal Graph

A causal graph, i.e., a directed acyclic graph (DAG), where edges represent causal relationships between variables. Taking cross-domain confounders \mathbf{C}_{cd} as an example, as illustrated in Fig. 2, they affect predicted interactions \hat{y} via two types of paths: $\mathbf{C}_{cd} \rightarrow \hat{y}$ and $\mathbf{C}_{cd} \rightarrow \mathbf{Z}_{sha} \rightarrow \mathbf{E}_u^* \rightarrow \hat{y}$. The first type of path reveals that \mathbf{C}_{cd} , even if not the primary cause, i.e., users’ true preferences, still have a direct positive impact on predicted interactions. The second type of path indicates that the negative impact of \mathbf{C}_{cd} on domain-shared user

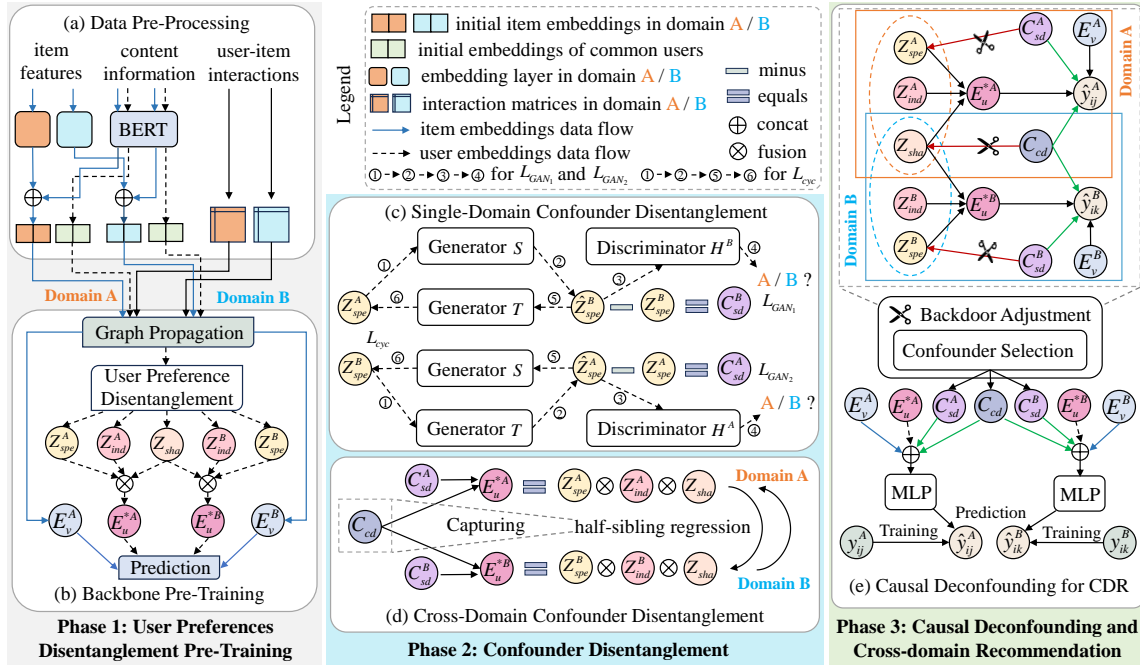


Fig. 3. The structure of our CD2CDR Framework. The symbols and arrows not shown in the legend are defined in Table I and Fig. 2.

preferences Z_{sha} induces confounding bias in both domains. Such confounding bias, in turn, skews comprehensive user preferences E_u^* , because Z_{sha} is an essential component for capturing E_u^* [53]. If the backdoor path $C_{cd} \rightarrow Z_{sha}$ is not blocked, C_{cd} will result in capturing biased comprehensive user preferences, thus yielding inaccurate recommendation results [19]. Similarly, single-domain confounders C_{sd} also have both positive and negative effects on predicted interactions and user preferences, respectively, thus the backdoor path $C_{sd} \rightarrow Z_{spe}$ in each domain should be blocked too.

Overall, the causal graph in Fig. 2 provides a detailed view of how user preferences, observed confounders, and user-item interactions are causally related in dual-target CDR. This helps in gaining a comprehensive understanding of user-item interactions by accounting for all influencing factors, ensuring more accurate recommendation performance.

C. Connection with Existing Works and Our Novel Insights

Our proposed CD2CDR is the first work to explicitly decouple observed cross-domain confounders and incorporate confounders' positive impacts into debiased comprehensive user preferences for dual-target CDR. Our study indicates that the proposed framework not only builds on existing works but also provides several novel insights [54]. Below, we analyze the remaining gaps in existing works and explain how our CD2CDR addresses these gaps and introduces novel insights:

- **Neglecting observed confounders in user preference modeling:** Existing approaches [29], [30] often emphasize decoupling essential components of user preferences to capture comprehensive user preferences, overlooking the impact of observed confounders on user decisions, which can lead to biased user preferences. In contrast, our CD2CDR addresses this gap by disentangling observed confounders and modeling the intricate causal relationships among such confounders, user preferences, and user-item interactions.

- **Suboptimal deconfounding due to lack of explicit decoupling of cross-domain confounders:** Existing approaches either use off-the-shelf features as confounders [47], [48] or neglect the need for decoupling cross-domain confounders [10], [11], resulting in suboptimal deconfounding performance. By contrast, our CD2CDR focuses on the explicit decoupling of both single-domain and cross-domain confounders, introducing a new perspective on deconfounding in cross-domain settings.
- **Overlooking the positive impacts of observed confounders:** Existing approaches [38], [39] typically aim to remove the negative impacts of observed confounders to obtain debiased comprehensive user preferences, but they often ignore the positive impacts of such confounders on predicted interactions. In contrast, by incorporating these positive impacts into debiased comprehensive user preferences, our CD2CDR can obtain a more comprehensive understanding of user-item interactions.

IV. THE PROPOSED MODEL

A. Overview of CD2CDR

To improve the recommendation performance in both domains, we propose a novel **Causal Deconfounding** framework via **Confounder Disentanglement** for dual-target **Cross-Domain Recommendation**, called CD2CDR. As depicted in Fig. 3, the framework can be divided into three phases, i.e., **Phase 1: User Preference Disentanglement Pre-Training**, **Phase 2: Confounder Disentanglement**, and **Phase 3: Causal Deconfounding and Cross-domain Recommendation**. In **Phase 1**, we obtain disentangled domain-independent and domain-specific user preferences in each domain and domain-shared user preferences by pre-training the backbone introduced in [53]. In **Phase 2**, we first extract the SDCs in each domain by bidirectionally transforming domain-specific user preferences decoupled in Phase 1. Then, we distill

confounding factors that jointly influence comprehensive user preferences in each of both domains as CDCs by adopting half-sibling regression [55]. In **Phase 3**, we utilize the backdoor adjustment to deconfound the observed confounders disentangled in **Phase 2**. Specifically, we design a confounder selection function to mitigate negative effects of such confounders on user preferences, thus recovering debiased comprehensive user preferences. We then incorporate the confounders' positive effects into such debiased preferences to predict user-item interactions via a multi-layer perception (MLP) in each domain.

B. Phase 1: User Preference Disentanglement Pre-Training

Accurate disentanglement of user preferences is vital to ensure the robustness of subsequent confounder disentanglement process. Since the method introduced in [53] excels at decoupling three essential components of user preferences for modeling comprehensive user preferences, our CD2CDR adopts it as the backbone for user preference disentanglement. To extract more accurate disentangled user preferences, we consider multi-source content information of users and items, e.g., user reviews and item details. Taking domain A as an example, for each categorical feature field of an item (e.g., brand and category), we distill a set of unique features, which are then encoded into vectors using either one-hot or multi-hot encoding. Next, these encoded vectors are concatenated to form the raw feature vector for each item. We then transform the raw feature vectors of items $\mathbf{E}_{vr}^A \in \mathbb{R}^{d_A}$ into the dense embeddings $\mathbf{E}_{vd}^A \in \mathbb{R}^d$ as follows:

$$\mathbf{E}_{vd}^A = \mathbf{W}_{rd}^A \mathbf{E}_{vr}^A, \quad (1)$$

where $\mathbf{W}_{rd}^A \in \mathbb{R}^{d_A \times d_d}$ is a trainable mapping matrix. d_d denotes the dimensionality of dense embeddings. Then, for a user u_i , we collect all the user's reviews into a user text document. For an item v_j , we collect its title and all reviews on the item into an item text document. Next, we adopt a pre-trained BERT [56] to map the documents of all users and items in the training set into user text embeddings \mathbf{E}_{ut}^A and item text embeddings \mathbf{E}_{vt}^A , respectively. Finally, we concatenate \mathbf{E}_{vd}^A and \mathbf{E}_{vt}^A to form combined item embeddings \mathbf{E}_{vc}^A . We then transform $\mathbf{E}_{ut}^A, \mathbf{E}_{vc}^A$ into fixed-size initial user embeddings \mathbf{E}_{ui}^A and initial item embedding \mathbf{E}_{vi}^A in domain A as follows:

$$\mathbf{E}_{ui}^A = \delta_u^A \mathbf{E}_{ut}^A, \quad \mathbf{E}_{vi}^A = \delta_v^A \mathbf{E}_{vc}^A, \quad (2)$$

where δ_u^A and δ_v^A are the mapping functions of MLP layers. Similarly, we can obtain initial user embeddings \mathbf{E}_{ui}^B and initial item embeddings \mathbf{E}_{vi}^B in domain B . We then use such initial embeddings and the interaction matrices as inputs to pre-train the backbone, thus we obtain domain-independent, domain-specific, and domain-shared user preferences, namely, \mathbf{Z}_{ind} , \mathbf{Z}_{spe} , and \mathbf{Z}_{sha} , and pre-trained item embeddings \mathbf{E}_v . By incorporating the above three components of user preferences using attention mechanism in accordance with DIDA-CDR [53], we can obtain comprehensive user preferences \mathbf{E}_u^* .

C. Phase 2: Confounder Disentanglement

Since user-item interactions are also influenced by observed confounders apart from comprehensive user preferences, we

propose to decouple SDCs and CDCs, as detailed in the following subsections.

1) Single-Domain Confounder Disentanglement: To explore the single-domain confounders, we utilize bi-directional domain transformation to decouple them from previously obtained domain-specific user preferences. If such SDCs are not identified and explicitly decoupled, their negative effects on domain-specific user preferences can hardly be eliminated. By contrast, if they are well disentangled, the causal deconfounding module can utilize backdoor adjustment to remove the confounding bias, thus obtaining debiased domain-specific user preferences. Inspired by CycleGAN [57], we devise a dual adversarial structure, which consists of two domain transformation generators and two discriminators, to disentangle SDCs in each domain. Specifically, we aim to learn two generators, i.e., $S(\cdot) : D^A \rightarrow D^B$ and $T(\cdot) : D^B \rightarrow D^A$, to transform domain-specific user preferences in each domain.

Taking domain B as an example, the generator $S(\cdot)$ takes the domain-specific user preferences \mathbf{Z}_{spe}^A of common users in D^A as inputs to generate $\hat{\mathbf{Z}}_{spe}^B = S(\mathbf{Z}_{spe}^A)$ that look similar to domain-specific user preferences in domain B , i.e., \mathbf{Z}_{spe}^B . However, if there are still differences between the simulated preferences $\hat{\mathbf{Z}}_{spe}^B$ and the original ones \mathbf{Z}_{spe}^B , such differences are not characteristics of domain-specific user preferences in domain B , but should be considered as SDCs [46]. To ensure that the generator $S(\cdot)$ is proficient at domain-specific preference simulation, we introduce a discriminator $H^B(\cdot)$ to recognize which domain the domain-specific user preferences come from. In the adversarial learning paradigm, the discriminator is expected to improve the ability to differentiate domain-specific user preferences in each domain to achieve better discriminative performance, while the generator is supposed to generate indistinguishable simulations of these domain-specific preferences to confuse such discriminator [58]. For training the generator $S(\cdot)$ and the corresponding discriminator $H^B(\cdot)$, we adopt the adversarial loss [59], which can be expressed as follows:

$$\begin{aligned} \mathcal{L}_{GAN1}(S, H^B, D^A, D^B) = & \mathbb{E}_{\mathbf{Z}_{spe}^B \sim \mathbb{P}^B} [\log H^B(\mathbf{Z}_{spe}^B)] \\ & + \mathbb{E}_{\mathbf{Z}_{spe}^A \sim \mathbb{P}^A} [\log(1 - H^B(S(\mathbf{Z}_{spe}^A)))], \end{aligned} \quad (3)$$

where \mathbb{E} is the expectation, and $\mathbb{P}^A, \mathbb{P}^B$ denote the feature distribution of domain A and domain B , respectively. Similarly, for training the generator $T(\cdot)$ and the corresponding discriminator $H^A(\cdot)$, we adopt the adversarial loss $\mathcal{L}_{GAN2}(T, H^A, D^B, D^A)$. However, relying solely on adversarial loss is insufficient to ensure that a user's domain-specific preferences remain aligned with the user's preferences after transformation. If transformed domain-specific user preferences no longer reflect the user's preferences, then such transformation becomes meaningless, serving merely to deceive the discriminator. Hence, the generators should maintain cycle consistency, i.e., $\mathbf{Z}_{spe}^A \rightarrow S(\mathbf{Z}_{spe}^A) \rightarrow T(S(\mathbf{Z}_{spe}^A)) \approx \mathbf{Z}_{spe}^A$, $\mathbf{Z}_{spe}^B \rightarrow T(\mathbf{Z}_{spe}^B) \rightarrow S(T(\mathbf{Z}_{spe}^B)) \approx \mathbf{Z}_{spe}^B$ during the training process (see \mathcal{L}_{cyc} in Fig. 3(c)). To this end, we apply a cycle consistency loss, which is represented as follows:

$$\begin{aligned} \mathcal{L}_{cyc}(S, T) = & \mathbb{E}_{\mathbf{Z}_{spe}^A \sim \mathbb{P}^A} [\|T(S(\mathbf{Z}_{spe}^A)) - \mathbf{Z}_{spe}^A\|_1] \\ & + \mathbb{E}_{\mathbf{Z}_{spe}^B \sim \mathbb{P}^B} [\|S(T(\mathbf{Z}_{spe}^B)) - \mathbf{Z}_{spe}^B\|_1]. \end{aligned} \quad (4)$$

Moreover, the total objective function for training the generators and discriminators can be formulated as follows:

$$\begin{aligned} \mathcal{L}_{sd}(S, T, H^A, H^B) = & \mathcal{L}_{GAN_1}(S, H^B, D^A, D^B) \\ & + \mathcal{L}_{GAN_2}(T, H^A, D^B, D^A) + \lambda \mathcal{L}_{cyc}(S, T), \end{aligned} \quad (5)$$

where λ controls the importance of cycle consistency loss relative to adversarial losses. Following the method introduced in [46], upon training completion, we calculate the differences between the domain-specific user preferences after transformation and the original ones as candidate single-domain confounders, which are defined as follows:

$$\hat{\mathbf{C}}_{sd}^A = T(\mathbf{Z}_{spe}^B) - \mathbf{Z}_{spe}^A, \quad \hat{\mathbf{C}}_{sd}^B = S(\mathbf{Z}_{spe}^A) - \mathbf{Z}_{spe}^B. \quad (6)$$

Recall the causal graph in Fig. 2(a), the influence of single-domain confounders \mathbf{C}_{sd} on domain-specific user preferences \mathbf{Z}_{spe} results in confounding bias, leading to inaccurate estimation of \mathbf{Z}_{spe} . For example, as depicted in Fig. 1(e), in the ‘purchase’ domain, a data-driven RS improperly perceives the ‘free shipping’ (i.e., an SDC), as Alice’s ‘purchase’ domain preference, resulting in biased recommendation. Since our well-trained generator excels at simulating Alice’s ‘purchase’ domain preferences based on her ‘add to favorite’ domain preferences, if there are still differences as per Eq. (6), this indicates such differences are not Alice’s ‘purchase’ domain preferences but rather SDCs independent of her preferences. Such SDCs (e.g., ‘free shipping’), previously entangled with Alice’s ‘purchase’ domain preferences, are decoupled through our SDC disentanglement process. Note that this process specifically targets biased domain-specific user preferences, because unbiased ones are not entangled with such SDCs. Thus, although this process decouples SDCs from biased domain-specific user preferences, this does not imply a causal relationship $\mathbf{Z}_{spe} \rightarrow \mathbf{C}_{sd}$ in the causal graph, because SDCs are not generated by such biased domain-specific user preferences. To distill representative SDCs and reduce redundancy, we apply K-means clustering on candidate single-domain confounders $\hat{\mathbf{C}}_{sd}^A$ (or $\hat{\mathbf{C}}_{sd}^B$) and choose J_{sd}^A (or J_{sd}^B) cluster centroids to form the potential SDC subspace \mathcal{C}_{sd}^A (or \mathcal{C}_{sd}^B).

2) Cross-Domain Confounder Disentanglement: In addition to SDCs, it is more important to identify confounding factors that simultaneously affect user-item interactions in both domains. Inspired by the method introduced in [46], we employ half-sibling regression to disentangle CDCs from the previously obtained comprehensive user preferences in both domains. Half-sibling regression excels at capturing the influence of confounding factors that simultaneously affect multiple observed variables [55], and thus it is well suited for decoupling CDCs in dual-target CDR. As illustrated in Fig. 2(a), $\mathbf{C}_{cd} \rightarrow \mathbf{E}_u^A$ and $\mathbf{C}_{cd} \rightarrow \mathbf{E}_u^B$ indicate that CDCs indirectly influence the comprehensive user preferences in each of both domains via $\mathbf{C}_{cd} \rightarrow \mathbf{Z}_{sha} \rightarrow \mathbf{E}_u^A$ and $\mathbf{C}_{cd} \rightarrow \mathbf{Z}_{sha} \rightarrow \mathbf{E}_u^B$. Therefore, we can apply half-sibling regression to decouple \mathbf{C}_{cd} from \mathbf{E}_u^A and \mathbf{E}_u^B (see Fig. 3(d)). Taking the regression from domain A to domain B as an example, our goal is to estimate a transformation matrix $\mathbf{W}^{A \rightarrow B}$ such that:

$$\mathbf{E}_u^B \approx \mathbf{E}_u^A \mathbf{W}^{A \rightarrow B}, \quad (7)$$

using ridge regression, and regression results are expressed as:

$$\mathbf{W}^{A \rightarrow B} = [(\mathbf{E}_u^A)^T \mathbf{E}_u^A + \alpha \mathbf{I}]^{-1} (\mathbf{E}_u^A)^T \mathbf{E}_u^B, \quad (8)$$

where α denotes the regularization parameter. We assume that \mathbf{E}_u^A and \mathbf{C}_{sd}^B are independent, because \mathbf{E}_u^A are comprehensive user preferences in domain A , while \mathbf{C}_{sd}^B are SDCs specific to domain B . When we estimate a transformation matrix $\mathbf{W}^{A \rightarrow B}$ to predict \mathbf{E}_u^B using \mathbf{E}_u^A , the influence of \mathbf{C}_{sd}^B on \mathbf{E}_u^B will not be captured. This is because \mathbf{E}_u^A are independent from \mathbf{C}_{sd}^B , and as a result, utilizing \mathbf{E}_u^A cannot predict \mathbf{C}_{sd}^B and the influence of \mathbf{C}_{sd}^B on \mathbf{E}_u^B . By contrast, the influence of \mathbf{C}_{cd} on \mathbf{E}_u^B will be captured, because \mathbf{C}_{cd} simultaneously affect \mathbf{E}_u^A and \mathbf{E}_u^B , which means the regression results will only capture \mathbf{C}_{cd} . Hence, the regression results can be identified as candidate cross-domain confounders:

$$\hat{\mathbf{C}}_{cd}^{A \rightarrow B} = \mathbf{E}_u^A \mathbf{W}^{A \rightarrow B}. \quad (9)$$

Similarly, we can obtain the regression results from domain B to domain A , denoted as $\hat{\mathbf{C}}_{cd}^{B \rightarrow A}$. For cross-domain confounders, K-means clustering is also employed on the candidate cross-domain confounders $\hat{\mathbf{C}}_{cd}^{A \rightarrow B}$ and $\hat{\mathbf{C}}_{cd}^{B \rightarrow A}$, with the J_{cd} cluster centroids forming the potential CDC subspace \mathcal{C}_{cd} .

D. Phase 3: Causal Deconfounding and Cross-Domain Recommendation

After the confounder disentanglement, we obtain the potential SDC subspaces \mathcal{C}_{sd}^A and \mathcal{C}_{sd}^B , and potential CDC subspace \mathcal{C}_{cd} . From a causal perspective, if the backdoor paths (i.e., $\mathbf{C}_{sd} \rightarrow \mathbf{Z}_{spe}$ and $\mathbf{C}_{cd} \rightarrow \mathbf{Z}_{sha}$) are not blocked, the observed confounders \mathbf{C} will simultaneously influence user preferences \mathbf{Z} and user-item interactions \mathbf{Y} (see Fig. 1(a)), and thus cause biased estimation of comprehensive user preferences. To this end, we perform the *do*-calculus intervention based on backdoor adjustment [60] to block the backdoor paths $\mathbf{C} \rightarrow \mathbf{Z}$ and enable our model to more accurately estimate the direct effect $\mathbf{Z} \rightarrow \mathbf{Y}$ (also see Fig. 1(a)). Formally, the conventional likelihood $P(\mathbf{Y}|\mathbf{Z})$ is defined as:

$$P(\mathbf{Y}|\mathbf{Z}) = \sum_c P(\mathbf{Y}|\mathbf{Z}, c)P(c|\mathbf{Z}), \quad (10)$$

where c denotes a specific confounder selected from the confounder space \mathcal{C} . By applying the *do*-calculus, we exclude all influences directed towards the intervened variable (i.e., \mathbf{Z}), and then we have:

$$\begin{aligned} P(\mathbf{Y}|do(\mathbf{Z})) &= \sum_c P(\mathbf{Y}|do(\mathbf{Z}), c)P(c|do(\mathbf{Z})) \\ &= \sum_c P(\mathbf{Y}|\mathbf{Z}, c)P(c). \end{aligned} \quad (11)$$

For brevity, the detailed proof of the transformations $P(\mathbf{Y}|do(\mathbf{Z}), c) = P(\mathbf{Y}|\mathbf{Z}, c)$ and $P(c|do(\mathbf{Z})) = P(c)$ is omitted, which can be found in [61]. In fact, transforming $P(c|do(\mathbf{Z}))$ into the prior probability of confounders $P(c)$ blocks backdoor paths $\mathbf{C} \rightarrow \mathbf{Z}$. As a result, $P(\mathbf{Y}|do(\mathbf{Z}))$ mainly focus on modeling the direct effect $\mathbf{Z} \rightarrow \mathbf{Y}$. Specifically, we implement the backdoor adjustment by modeling $P(\mathbf{Y}|\mathbf{Z}, c)$ with an interaction prediction network, which is expressed as follows:

$$P(\mathbf{Y}|do(\mathbf{Z})) = \mathbb{E}_c[P(\mathbf{Y}|\mathbf{Z}, c)] = \mathbb{E}_c[f(\mathbf{E}_u^*, \mathbf{E}_v, \mathbf{c})], \quad (12)$$

where $f(\cdot)$ denotes a neural network, namely, MLP, to predict the probabilities of user-item interactions [62]. \mathbf{E}_u^* and \mathbf{E}_v are comprehensive user preferences and pre-trained item embeddings obtained by the backbone in Phase 1, respectively. In other words, based on two subspaces of disentangled observed confounders in domain A and domain B , i.e., $\mathcal{C}^A = \mathcal{C}_{sd}^A \cup \mathcal{C}_{cd}$ and $\mathcal{C}^B = \mathcal{C}_{sd}^B \cup \mathcal{C}_{cd}$, we apply backdoor adjustment to rectify the biased recommendations in each domain using Eq. (12). Moreover, since the decoupled observed confounders are incorporated as part of the input to the MLP, the direct influence of such confounders on user-item interactions $C \rightarrow Y$ is also considered. In addition, inspired by the approach in [46], we devise a confounder selection function to effectively control the decoupled confounders for more accurate deconfounding.

Taking domain A as an example, the confounder selection function is defined as follows:

$$\phi(\mathbf{E}_u^A, \mathbf{E}_v^A, \mathbf{c}) = \frac{\exp(\mathbf{W}_u^A \mathbf{E}_u^A \cdot \mathbf{W}_{uc}^A \mathbf{c})}{2 \sum_{\mathbf{c}'} \exp(\mathbf{W}_u^A \mathbf{E}_u^A \cdot \mathbf{W}_{uc}^A \mathbf{c}')} + \frac{\exp(\mathbf{W}_v^A \mathbf{E}_v^A \cdot \mathbf{W}_{vc}^A \mathbf{c})}{2 \sum_{\mathbf{c}'} \exp(\mathbf{W}_v^A \mathbf{E}_v^A \cdot \mathbf{W}_{vc}^A \mathbf{c}')}, \quad (13)$$

where \mathbf{c}' denotes any confounder selected from confounder subspace \mathcal{C}^A and \cdot is the dot product. $\mathbf{W}_u^A, \mathbf{W}_{uc}^A, \mathbf{W}_v^A, \mathbf{W}_{vc}^A$ are trainable matrices for embedding transformation. We then formulate the expectation $\mathbb{E}_c[f(\mathbf{E}_u^*, \mathbf{E}_v, \mathbf{c})]$ as follows:

$$\mathbb{E}_c[f(\mathbf{E}_u^*, \mathbf{E}_v, \mathbf{c})] = f(\mathbf{Q}_{in}^A) = f[\mathbf{W}_{fc}(\mathbf{E}_u^A || \mathbf{E}_v^A || \sum_c p(c) \mathbf{c} \phi(\mathbf{E}_u^A, \mathbf{E}_v^A, \mathbf{c}))], \quad (14)$$

where \mathbf{W}_{fc} is the weight matrix of the fully connected (FC) layer and $||$ is the concatenation operator. In practice, we assume a uniform distribution for the prior probability $p(c)$. In addition, $\mathbf{Q}_{in}^A = \mathbf{W}_{fc}(\mathbf{E}_u^A || \mathbf{E}_v^A || \sum_c p(c) \mathbf{c} \phi(\mathbf{E}_u^A, \mathbf{E}_v^A, \mathbf{c}))$ denotes the input for MLP in domain A . Moreover, the predicted interaction \hat{y}_{ij}^A between an user u_i and an item v_j in domain A is represented as follows:

$$\hat{y}_{ij}^A = \delta_{out}^A(\delta_l^A(\dots \delta_2^A(\delta_1^A(\mathbf{Q}_{in}^A))\dots)), \quad (15)$$

where δ_l^A is the mapping function for l -th MLP layer, and there are l MLP layers including δ_{out}^A in domain A . Similarly, the predicted interaction \hat{y}_{ik}^B in domain B can be obtained.

The essence of our causal deconfounding module lies in blocking the backdoor paths $C \rightarrow Z$, allowing the model to concentrate on the direct effects of users' true preferences on the predicted interactions $Z \rightarrow Y$, and disregard the interference of confounders on these preferences. Specifically, the confounder selection function assigns different weights to the potential observed confounders, mitigates the effects of those irrelevant or harmful confounders to the prediction task, and enhances the direct effects of beneficial confounders on predicted interactions. Therefore, this module enables the model to eliminate the negative effects of such observed confounders to learn debiased comprehensive user preferences, and preserve the positive effects of these confounders on predicted interactions, thereby achieving a more comprehensive understanding of user-item interactions in both domains. Finally, we employ cross-entropy loss to fine-tune the user preference disentanglement backbone $g(\cdot)$ and the interaction

prediction network $f(\cdot)$. To be specific, the final objective function in domain A can be defined as follows:

$$g^*, f^* = \arg \min_{g, f} \sum_{y \in \mathcal{Y}^A + \cup \mathcal{Y}^A -} \ell(\hat{y}, y), \quad (16)$$

where \hat{y} and y are the predicted interaction and corresponding observed interaction, respectively. $\ell(\hat{y}, y)$ denotes the cross-entropy loss function. \mathcal{Y}^{A+} denotes the observed interaction set, and \mathcal{Y}^{A-} corresponds to a specific quantity of negative samples, which are randomly selected from unseen user-item interaction set in domain A to mitigate the over-fitting. During the fine-tuning process, $g(\cdot)$ serves as the backbone, with the original prediction module being replaced by the interaction prediction network $f(\cdot)$. Likewise, we can obtain the objective function and predicted user-item interaction \hat{y}_{ik}^B in domain B .

E. Time Complexity Analysis

Our CD2CDR mainly focuses on four modules: (1) Graph Propagation, (2) User Preference Disentanglement, (3) Confounder Disentanglement, and (4) Causal Deconfounding and Cross-domain Recommendation. While the first two modules are part of backbone model [53], the latter two constitute our novel framework. For simplicity and consistency, we assume that all embedding dimensions are d and the number of layers in each network structure within each module is L [63]. The details of analysis for each module are shown in Appendix A.

Overall, the time complexity of our CD2CDR can be approximated as $O(mnd^2(J + L))$, where J is the number of cluster centroids, and m and n are the number of users and items, respectively. This approximation is based on combining the time complexities of all four modules and simplifying by focusing on the dominant terms. The overall time complexity exhibits a non-linear relationship with the number of users, items, observed confounders, and embedding dimensions.

V. EXPERIMENTS AND ANALYSIS

Extensive experiments are conducted on five real-world datasets to answer the following four research questions:

- **RQ1.** How does our model perform in comparison with state-of-the-art baseline models (see Section V-B)?
- **RQ2.** How do different components, namely, confounder disentanglement, causal deconfounding and cycle consistency loss, influence the recommendation accuracy of our model (see Section V-C)?
- **RQ3.** How do different backbone models impact the recommendation accuracy of our model (see Section V-D)?
- **RQ4.** How do different hyper-parameter settings affect the recommendation accuracy of our model (see Section V-E)?

A. Experimental Settings

1) **Experimental Datasets:** Semantic information, such as item titles containing details about free shipping, sales promotion, category, and brand, helps to disentangle user preferences and observed confounders. In e-commerce scenarios, semantic information is easily accessible and crucial for gaining a more comprehensive understanding of user-item interactions.

TABLE II
THE STATISTICAL DATA FOR THREE DUAL-TARGET CDR TASKS.

Tasks	Datasets	#Users	#Items	#Interactions	Density
Task #1	Tmall-Favorite	25,434	99,237	500,876	0.020%
	Tmall-Purchase	25,434	28,817	55,057	0.008%
Task #2	Tmall-Favorite	39,657	104,496	807,493	0.019%
	Tmall-Cart	39,657	44,172	354,499	0.020%
Task #3	Amazon-Elec	15,761	51,447	224,689	0.027%
	Amazon-Cloth	15,761	48,781	133,609	0.017%

Therefore, to validate the recommendation accuracy of our CD2CDR, we select two real-world e-commerce datasets that provide rich semantic information, ratings, reviews and item metadata, namely, Rec-Tmall¹ dataset [64] and Amazon dataset [29]. For Amazon dataset, we choose two relevant domains, namely, Amazon-Electronics and Amazon-Cloth. Similarly, for Rec-Tmall dataset, we select three relevant applications as domains, namely, Add to Favorite, Purchase, and Add to Cart². In Tmall-Favorite, most users enjoy browsing items without the specific intention of purchasing. In Tmall-Purchase and Tmall-Cart, users prefer recommendations based on items they have previously purchased [10].

2) **Experimental Tasks:** For the above five subsets, we first transform ratings into implicit feedback, and then construct three dual-target CDR tasks with fully overlapping user sets. These tasks are chosen to test the model’s ability to handle diverse dual-target CDR scenarios by covering different user interactions and preferences. Specifically, we construct the following tasks: (1) Tmall-Favorite and Tmall-Purchase, (2) Tmall-Favorite and Tmall-Cart, and (3) Amazon-Elec and Amazon-Cloth. These tasks are designed to represent various e-commerce scenarios, ensuring that our model can effectively address different types of user interactions and item features.

For Task #1, users and items with fewer than 20 interactions are removed from Tmall-Favorite, and those with fewer than 5 interactions are filtered out from Tmall-Purchase. For the Task #2 and Task #3, users and items with fewer than 20 interactions in Task #2 and those with fewer than 5 interactions in Task #3 are filtered out. In line with the preprocessing operation taken for the two Amazon subsets in DisenCDR [29], we also conduct the same operation on three Rec-Tmall subsets to remove the cold-start item entry for testing. The statistical data for the above three tasks are expressed in Table II.

3) **Parameter Settings:** The settings of our backbone DIDA-CDR are consistent with those listed in its original paper [53], including the number of GCN layers, embedding dimension and information fusion approach, etc. In the interaction prediction network, the structure is $e \rightarrow 32 \rightarrow 16 \rightarrow q$, where e is the combined size after the mapping of FC layer in Eq. (14), and q is the output size, i.e., the dimension of latent factors. We vary e in the range of $\{64, 128\}$ and q in the range of $\{8, 16\}$, and finally set $e = 128$ and $q = 8$. The initial parameters for all the above layers are set following a Gaussian distribution $X \sim \mathcal{N}(0, 0.01)$. In line with the approach used in GA-DTCDR [65], for each observed interaction, we randomly select 7 non-interacted items to serve as negative

examples. For a fair comparison, we employ grid search to fine-tune the parameters of all models. Specifically, we select the learning rate in $\{0.01, 0.005, 0.001, 0.0005, 0.0001\}$. Moreover, we adopt the Adam optimizer [66] for all models with a batch size of 1024. Furthermore, we investigate the weight of cycle consistency loss λ in $\{0.1, 1, 2, 5, 10\}$, and the regularization parameter α in $\{0.1, 1, 10, 20, 50\}$. We keep the number of cluster centroids $J_{sd}^A = J_{sd}^B = J_{cd}$ and vary them in $\{2, 5, 10, 20, 50\}$. The influence of the above parameters on our CD2CDR is particularly discussed in Section V-E³.

4) **Model Training:** Since our CD2CDR can be divided into three phases, we first pre-train the backbone of our model with 50 epochs⁴ to obtain disentangled user preferences and comprehensive user preferences. Next, we train the generators and discriminators in the dual adversarial structure with 30 epochs to decouple SDCs, apply half-sibling regression, a computational method inherently without a training process [55], to decouple CDCs, and then save cluster centroids of both SDCs and CDCs. Finally, we replace the prediction module in the backbone with the interaction prediction network to fine-tune the overall CD2CDR with 20 epochs. During each epoch, we shuffle and split the training data for both domains into batches. We then iterate through the batches, training on domain A and domain B in parallel. This approach allows the model to learn from both domains within the same epoch, ensuring that the model parameters are updated based on information from both domains. This form of joint learning helps improve the generalization performance across domains. Note that Eq. (5) and Eq. (16) are not optimized jointly. This is because observed confounders are no longer entangled with debiased user preferences after deconfounding, the joint optimization of Eq. (5) and Eq. (16) for decoupling observed confounders from debiased user preferences becomes redundant. For a fair comparison, other baselines are trained for 100 epochs to confirm their convergence.

5) **Evaluation Metrics:** Given the widespread use of leave-one-out approach in baselines, e.g., GA-DTCDR [65] and DisenCDR [29], we adopt it as well to validate the recommendation accuracy of our CD2CDR and baselines. Moreover, the test set is created by the final interaction for each user, while the training set is formed by the remaining interaction records. In line with the methods introduced in [16], [29], for every interaction in the test set, we randomly select 999 non-interacted items as negative samples for the test user, and then predict scores for a total of 1000 items to perform ranking. The leave-one-out method mainly uses Hit Ratio (HR) and Normalized Discounted Cumulative Gain (NDCG), which are commonly adopted in ranking evaluations [25]. In our experiments, these metrics are applied to validate the recommendation accuracy within top-10 rankings, and all experiments are conducted five times with average results reported in this paper.

6) **Comparison Methods:** We choose thirteen state-of-the-art baseline models to conduct a comparison against the

¹<https://tianchi.aliyun.com/dataset/140281>

²For brevity, we refer to these subsets as Tmall-Favorite, Tmall-Purchase, Tmall-Cart, Amazon-Elec, and Amazon-Cloth, respectively in subsequent discussions.

³Due to space limitation, we only list the more critical discussions regarding the number of cluster centroids and omit the performance comparison details for λ and α , which are set as $\lambda = 1$ and $\alpha = 1$ in the experiments.

⁴The number of training epochs for each phase is chosen in $\{10, 20, 30, 40, 50\}$.

TABLE III
THE COMPARISON OF THE BASELINES AND OUR PROPOSED MODEL.

Model		Embedding Strategy	Main Idea
Baselines	Single-Domain Recommendation (SDR)	NGCF [67]	Devising an embedding propagation layer to encode the collaborative signal
		LightGCN [68]	Designing a simplified GCN using linear message propagation for RSs
	Single-Target Cross-Domain Recommendation (CDR)	BPR_EMCDR [69]	Mapping the latent factors of common users/items for knowledge transfer
		BPR_DCDCSR [70]	Considering the rating sparsity degrees of individual users and items
	Debiasing Dual-Target CDR	SCDGN [15]	Distilling unbiased graph knowledge and learning debiasing vectors
		CDRIB [16]	Designing two information bottleneck regularizers for debiasing
		IPSCDR [10]	Eliminating selection bias and transferring debiased user preferences
	Disentanglement-Based Dual-Target CDR	GA-DTCDR [65]	Generating and effectively combining more representative embeddings
		DisenCDR [29]	Developing two mutual-information-based disentanglement regularizers
		CausalCDR [71]	Using causal embeddings to model the joint distribution of user interactions
		GDCCDR [72]	Using disentangled graph for disentanglement and personalized transfer
		HJID [73]	Devising a hierarchical subspace disentanglement method for latent factors
Our model	Deconfounding Dual-Target CDR	DIDA-CDR [53]	Decoupling three components to capture comprehensive user preferences
		CD2CDR	Disentangling fine-grained observed confounders and deconfounding

TABLE IV
COMPARATIVE PERFORMANCE ANALYSIS (%) OF DIFFERENT METHODS IN ALL THREE TASKS USING HR@10 AND NDCG@10 AS EVALUATION METRICS [65]. FOR EXPERIMENTAL RESULTS, THE BEST RESULTS ARE HIGHLIGHTED IN BOLD AND THE RESULTS OF BEST-PERFORMING BASELINE MODEL ARE UNDERLINED (* DENOTES $p < 0.05$ IN THE PAIRED T-TEST BETWEEN THE BEST-PERFORMING BASELINE MODEL AND CD2CDR) [53].

Datasets	SDR Baselines				Single-Target CDR Baselines				Debiasing Dual-Target CDR Baselines					
	NGCF		LightGCN		BPR_EMCDR		BPR_DCDCSR		SCDGN		CDRIB		IPSCDR	
	HR	NDCG	HR	NDCG	HR	NDCG	HR	NDCG	HR	NDCG	HR	NDCG	HR	NDCG
Tmall-Favorite	12.39	6.27	12.62	6.35	-	-	-	-	15.07	8.16	15.9	8.62	17.14	9.38
Tmall-Purchase	6.46	4.01	6.74	4.06	5.31	3.56	5.88	3.73	8.73	4.75	9.56	5.17	10.51	5.39
Tmall-Favorite	12.48	6.29	12.81	6.43	-	-	-	-	15.14	8.21	16.22	9.04	17.43	9.47
Tmall-Cart	10.04	5.23	10.85	5.58	8.79	4.87	9.46	5.11	12.82	6.48	13.98	7.51	15.05	8.02
Amazon-Elec	21.85	12.36	21.73	11.61	-	-	-	-	24.69	13.85	25.06	14.34	26.78	15.19
Amazon-Cloth	11.62	6.18	12.04	6.22	10.69	5.47	11.44	6.15	15.19	8.24	16.67	9.18	18.26	9.93

Datasets	Disentanglement-Based Dual-Target CDR Baselines										Deconfounding Dual-Target CDR (our)		Improvement	
	GA-DTCDR		DisenCDR		CausalCDR		GDCCDR		HJID		DIDA-CDR		CD2CDR	
	HR	NDCG	HR	NDCG	HR	NDCG	HR	NDCG	HR	NDCG	HR	NDCG	HR	NDCG
Tmall-Favorite	14.87	7.82	15.34	8.25	15.96	8.69	16.24	9.05	16.45	9.12	16.60	9.14	18.01*	9.87*
Tmall-Purchase	8.44	4.53	9.01	4.94	9.17	5.03	9.65	5.19	9.88	5.22	10.03	5.28	11.38*	6.12*
Tmall-Favorite	14.91	8.05	15.39	8.53	16.25	9.10	16.53	9.13	16.79	9.19	17.02	9.26	18.35*	9.98*
Tmall-Cart	12.66	6.38	13.13	6.81	13.56	7.18	14.21	7.56	14.43	7.60	14.56	7.71	16.37*	9.06*
Amazon-Elec	24.79	13.87	24.53	14.02	25.14	14.47	25.69	14.58	25.94	14.71	26.12	14.83	28.11*	16.24*
Amazon-Cloth	14.58	7.64	15.81	8.56	15.93	8.65	16.72	9.16	17.27	9.42	17.75	9.70	19.62*	10.87*

proposed CD2CDR. We then categorize the thirteen baseline models into four groups: (I) Single-Domain Recommendation (SDR), (II) Single-Target Cross-Domain Recommendation (CDR), (III) Debiasing Dual-Target CDR, and (IV) Disentanglement-Based Dual-Target CDR. To the best of our knowledge, our CD2CDR is the first Deconfounding Dual-Target CDR model in the literature. Thus, we select three representative Debiasing Dual-Target CDR approaches as alternatives for Deconfounding Dual-Target CDR baselines. Moreover, although there are some methods that identify unobserved domain-specific confounders and even unobserved general confounders, or utilize backdoor adjustment in the single-domain manner, they are not selected as baseline models. This is because they focus on different settings, i.e., domain generalization [11], [74], CDSR [38], [39], [75], click-through rate (CTR) prediction [76], [77] and different item groups [8], [9], respectively, from our model. Furthermore, in Table III, we present an in-depth analysis of embedding strategies and main ideas of thirteen baselines and our CD2CDR. Detailed descriptions of these baselines are provided in Appendix B.

Overall, our baselines cover both single-domain and various types of cross-domain recommendation models. In the experiments, we use our CD2CDR framework to extend all the above Disentanglement-Based Dual-Target CDR baselines. The experimental results (see Section V-D) demonstrate that our CD2CDR is highly extendable and compatible with most off-the-shelf disentanglement-based dual-target CDR backbone models, making it suitable for a wide range of CDR scenarios.

B. Performance Comparison (for RQ1)

Table IV displays a comparative analysis of the performance⁵ of different methods across all three tasks using HR@10 and NDCG@10 as evaluation metrics. It is worth mentioning that the Single-Target CDR baseline models are trained in both domains, but only their results in the data-sparsier domain are reported, because they are designed to enhance the recommendation accuracy in the data-sparsier domain. We can observe from Table IV:

- (1) Our CD2CDR improves Disentanglement-Based Dual-Target CDR baselines by an average of 15.43% and 17.11% w.r.t. HR@10 and NDCG@10, respectively. This is because, in addition to the user preference disentanglement, we adopt the confounder disentanglement, which effectively decouples observed SDCs and CDCs, thus gaining a more comprehensive understanding of user-item interactions. By decoupling these confounders, we account for the fact that user interactions are not solely driven by their true preferences but also by observed confounders. Such confounders' positive influences can be secondary causes for user interactions, while their negative influences will result in capturing biased comprehensive user preferences. Effectively decoupling such observed confounders allows us to consider a more comprehensive range of factors

⁵We only display experimental results when the embedding dimension $d = 64$ in Table IV due to space limitation. For other values of d that are not shown, similarly, our CD2CDR also significantly outperforms other baselines.

affecting user-item interactions, thereby achieving better recommendation performance in both domains;

- (2) Our CD2CDR improves Debiasing Dual-Target CDR baselines by an average of 14.04% and 15.84% w.r.t. HR@10 and NDCG@10, respectively. This demonstrates that deconfounding the observed confounders in each of both domains effectively benefits the prediction of user-item interactions in dual-target CDR;
- (3) Our CD2CDR improves the best-performing baseline, i.e., IPSCDR [10], which is implemented with the same backbone as our model. Specifically, our CD2CDR outperforms IPSCDR with an average increase of 6.64% and 8.92% w.r.t. HR@10 and NDCG@10, respectively. This is because our CD2CDR particularly takes observed CDCs into consideration and our causal deconfounding module can not only eliminate observed confounders' negative effects on user preferences, but also preserve their positive effects on predicted interactions.

C. Ablation Study (for RQ2)

To highlight the significance of each component in enhancing the recommendation accuracy of model, we reconstruct our CD2CDR into four variants and perform an ablation study for all three tasks.

1) **Impact of Confounder Disentanglement:** We modify our proposed CD2CDR to form two variants, namely **CD2CDR_Cross** and **CD2CDR_Single**, by removing the SDC disentanglement and CDC disentanglement, respectively. From Table V, we can observe that with SDC disentanglement module, our proposed CD2CDR outperforms **CD2CDR_Cross** with an average improvement of 6.24%. This shows that the dual adversarial structure can effectively disentangle observed SDCs, and SDCs play an important role in predicting user-item interactions in each domain. In addition, our proposed CD2CDR improves **CD2CDR_Single** by an average increase of 4.91%. This indicates that half-sibling regression is well suited for decoupling observed CDCs, which are essential factors for achieving a comprehensive understanding of user-item interactions in both domains. Overall, our confounder disentanglement module can explicitly decouple more accurate observed confounders, especially the CDCs, thus enable our model to obtain better recommendation performance via accurate causal deconfounding.

2) **Impact of Causal Deconfounding:** Moreover, another variant, namely **CD2CDR_Coarse**, directly incorporates decoupled observed confounders with biased comprehensive user preferences in each domain and does not include the causal deconfounding module. From Table V, we can observe that without the causal deconfounding module, the recommendation accuracy of **CD2CDR_Coarse** drops by 24.54% on average, making it less effective compared to the Debiasing Dual-Target CDR baselines. This shows that the causal deconfounding module indeed helps the model control the negative effects of SDCs and CDCs on user preferences. By recovering debiased comprehensive user preferences and then incorporating the positive effects of SDCs and CDCs into such preferences, the module enables the model to obtain the better recommendation accuracy in both domains.

TABLE V
ABLATION STUDY OF DIFFERENT COMPONENTS IN OUR CD2CDR ACROSS THREE DUAL-TARGET CDR TASKS. THE BEST RESULTS ARE HIGHLIGHTED IN BOLD.

Variants	Tmall-Favorite		Tmall-Purchase	
	HR	NDCG	HR	NDCG
CD2CDR_Cross	17.25	9.41	10.67	5.40
CD2CDR_Single	17.48	9.56	10.82	5.53
CD2CDR_Coarse	15.03	8.14	8.68	4.69
CD2CDR_Cycle	17.86	9.70	11.22	6.04
CD2CDR	18.01	9.87	11.38	6.12

Variants	Tmall-Favorite		Tmall-Cart	
	HR	NDCG	HR	NDCG
CD2CDR_Cross	17.64	9.59	15.21	8.25
CD2CDR_Single	17.85	9.69	15.56	8.61
CD2CDR_Coarse	15.11	8.16	12.75	6.43
CD2CDR_Cycle	18.23	9.89	16.18	9.01
CD2CDR	18.35	9.98	16.37	9.06

Variants	Amazon-Elec		Amazon-Cloth	
	HR	NDCG	HR	NDCG
CD2CDR_Cross	26.83	15.23	18.32	9.96
CD2CDR_Single	26.97	15.32	18.44	10.01
CD2CDR_Coarse	24.48	13.79	14.76	7.68
CD2CDR_Cycle	27.94	16.15	19.37	10.58
CD2CDR	28.11	16.24	19.62	10.87

3) **Impact of Cycle Consistency Loss:** In addition, we construct another variant, namely **CD2CDR_Cycle**, by removing the cycle consistency loss in the SDC disentanglement module. From Table V, we can observe that our CD2CDR improves **CD2CDR_Cycle** by an average of 2.21%. This demonstrates that the cycle consistency loss effectively preserves users' domain-specific preferences during the transformation process, ensuring the transformed preferences accurately reflect the original user preferences rather than merely deceiving the discriminator. By incorporating the cycle consistency loss to stabilize the adversarial loss, our model can more accurately disentangle single-domain confounders, providing strong support for explicitly considering the impact of observed confounders on user preferences and user-item interactions.

D. Impact of Different Backbones (for RQ3)

Since our CD2CDR can be easily combined with disentanglement-based dual-target CDR backbone models, in addition to DIDA-CDR [53], we select all the other representative and state-of-the-art models from this group as backbones to form the following five variants, namely, **GA-DTCDR_CD2CDR**, **DisenCDR_CD2CDR**, **CausalCDR_CD2CDR**, **GDCCDR_CD2CDR** as well as **HJID_CD2CDR**. Our aim is to demonstrate the flexibility and effectiveness of our CD2CDR by integrating it with various representative and state-of-the-art disentanglement-based dual-target CDR backbone models, thereby highlighting its generalizability and extendability across diverse CDR scenarios. The performance comparison of our CD2CDR, and its five variants with corresponding backbones is shown

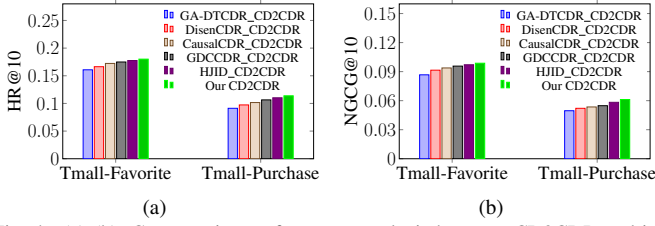


Fig. 4. (a)-(b): Comparative performance analysis between CD2CDR and its five variants with different backbones.

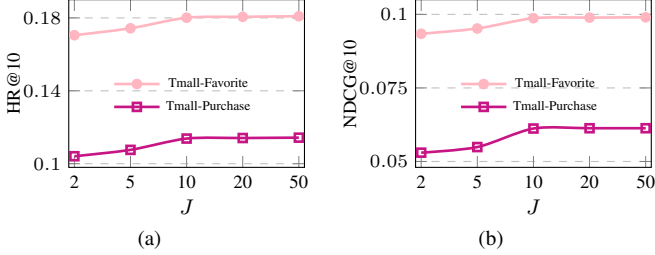


Fig. 5. (a)-(b): Impact of the number of cluster centroids J .

in Fig. 4⁶. We find that when our model employs DIDA-CDR as the backbone, it improves the above five variants, namely, **GA-DTCR_CD2CDR**, **DisenCDR_CD2CDR**, **CausalCDR_CD2CDR**, **GDCCDR_CD2CDR** as well as **HJID_CD2CDR** by an average of 16.87%, 11.42%, 7.74%, 5.09% and 2.34%, respectively. This improvement can be attributed to the ability of DIDA-CDR to effectively decouple three components of user preferences for modeling more accurate comprehensive user preferences. Notably, the ability of DIDA-CDR aligns well with the requirements of our CD2CDR, which relies on this precise disentanglement to accurately decouple observed confounders. In addition, our model, when combined with various backbones, consistently outperforms these backbones in their original form with an average improvement of 8.98% and 8.56% w.r.t. HR@10 and NDCG@10, respectively. This not only demonstrates the superior efficacy of our CD2CDR in improving the recommendation performance in both domains, but also shows its generalizability to various CDR models.

E. Parameter Sensitivity (for RQ4)

To explore the impact of number of cluster centroids J on the efficacy of our proposed CD2CDR, we keep $J_{sd}^A = J_{sd}^B = J_{cd}$ and vary them in $\{2, 5, 10, 20, 50\}$. The corresponding experimental results are depicted in Fig. 5. We can observe that as J increases, the recommendation performance initially improves but gradually plateaus beyond 10. This suggests that there is a threshold for J , which may vary in different datasets. Beyond this threshold, additional cluster centroids do not significantly improve the recommendation performance. In other words, once J reaches this threshold, the potential confounders represented by these cluster centroids are comprehensive enough for effective deconfounding. With the aim of achieving a balance between model complexity and recommendation accuracy, we finally set $J_{sd}^A = J_{sd}^B = J_{cd} = 10$ in all three tasks.

⁶Owing to constraints in space, Fig. 4 and Fig. 5 solely present the experimental results for Task #1, with similar trends observed in the other unshown tasks.

In particular, the comprehensive confounder disentanglement significantly contributes to more accurate estimation of Eq. (12). More importantly, the experimental results show that our confounder disentanglement module can form effective confounder spaces, where even basic clustering techniques can easily identify key confounders, thereby yielding promising deconfounding results.

F. Discussion

The experimental results indicate that (1) Our CD2CDR consistently improves thirteen baselines. The improvements are primarily due to our proposed confounder disentanglement module and causal deconfounding module. The confounder disentanglement module, designed with the dual adversarial structure and half-sibling regression, efficiently decouples observed SDCs and CDCs. The causal deconfounding module uses backdoor adjustment to deconfound such decoupled observed confounders and incorporates their positive effects into debiased comprehensive user preferences, enhancing recommendation performance in both domains. By contrast, the baseline models either ignore cross-domain confounders or only consider the negative effects of observed confounders, limiting their ability to achieve a comprehensive understanding of user-item interactions and resulting in downgrade recommendation performance; (2) CD2CDR offers a certain degree of interpretability, tailored for dual-target CDR to deconfound observed SDCs and CDCs from a causal perspective. Through comprehensive ablation studies, we highlight the impact of each module in accurately modeling the causal relationships among observed confounders, user preferences, and user-item interactions; (3) Our CD2CDR is a robust dual-target CDR model capable of integrating with various state-of-the-art disentanglement-based backbone models, thereby highlighting its generalizability and extendability across diverse CDR scenarios. As demonstrated in Section V-D, we combined our CD2CDR framework with several state-of-the-art disentanglement-based dual-target CDR backbones, resulting in an average improvement of 8.98% and 8.56% w.r.t. HR@10 and NDCG@10, respectively. This indicates that with our framework, existing disentanglement-based dual-target CDR models can be extended for effective deconfounding, which is influential in developing more advanced CDR models.

VI. CONCLUSION AND FUTURE WORK

In this paper, we have proposed a novel Causal Deconfounding framework via Confounder Disentanglement for dual-target CDR, called CD2CDR. CD2CDR not only effectively decouples observed single-domain and cross-domain confounders, but also preserves the positive direct effects of such observed confounders on predicted interactions and eliminates their negative effects on capturing comprehensive user preferences, thereby enhancing the recommendation accuracy in both domains simultaneously. Moreover, we have conducted extensive experiments on five real-world datasets, which demonstrates that our CD2CDR significantly outperforms the state-of-the-art methods.

A limitation of this work is the focus on a dual-domain scenario, which does not fully address the multi-domain causal effects present in real-world applications. In the future, we intend to extend our framework to account for multi-domain causal impacts to better reflect real-world scenarios and enhance scalability to large-scale datasets. Meanwhile, we plan to explore unobserved confounders, and further mitigate other types of biases apart from confounding bias.

REFERENCES

- [1] F. Zhu, C. Chen, Y. Wang, G. Liu, and X. Zheng, “DTCDR: A framework for dual-target cross-domain recommendation,” in *CIKM*, 2019, pp. 1533–1542.
- [2] C. Gao, Y. Zheng, W. Wang, F. Feng, X. He, and Y. Li, “Causal inference in recommender systems: A survey and future directions,” *ACM TOIS*, vol. 42, no. 4, pp. 1–32, 2022.
- [3] Y. Zhu, J. Ma, and J. Li, “Causal inference in recommender systems: A survey of strategies for bias mitigation, explanation, and generalization,” *arXiv preprint arXiv:2301.00910*, 2023.
- [4] A. Wu, K. Kuang, R. Xiong, and F. Wu, “Instrumental variables in causal inference and machine learning: A survey,” *arXiv preprint arXiv:2212.05778*, 2022.
- [5] H. Luo, F. Zhuang, R. Xie, H. Zhu, D. Wang, Z. An, and Y. Xu, “A survey on causal inference for recommendation,” *The Innovation*, vol. 5, no. 2, p. 100590, 2024.
- [6] S. C. Gowda, S. Joshi, H. Zhang, and M. Ghassemi, “Pulling up by the causal bootstraps: Causal data augmentation for pre-training debiasing,” in *CIKM*, 2021, pp. 606–616.
- [7] X. Zhu, Y. Zhang, X. Yang, D. Wang, and F. Feng, “Mitigating hidden confounding effects for causal recommendation,” *IEEE TKDE*, pp. 1–12, 2024.
- [8] Y. Zhang, F. Feng, X. He, T. Wei, C. Song, G. Ling, and Y. Zhang, “Causal intervention for leveraging popularity bias in recommendation,” in *SIGIR*, 2021, pp. 11–20.
- [9] W. Wang, F. Feng, X. He, X. Wang, and T.-S. Chua, “Deconfounded recommendation for alleviating bias amplification,” in *KDD*, 2021, pp. 1717–1725.
- [10] S. Li, L. Yao, S. Mu, W. X. Zhao, Y. Li, T. Guo, B. Ding, and J.-R. Wen, “Debiasing learning based cross-domain recommendation,” in *KDD*, 2021, pp. 3190–3199.
- [11] Y. Zhang, Y. Shen, D. Wang, J. Gu, and G. Zhang, “Connecting unseen domains: Cross-domain invariant learning in recommendation,” in *SIGIR*, 2023, pp. 1894–1898.
- [12] Q. Li, X. Wang, Z. Wang, and G. Xu, “Be causal: De-biasing social network confounding in recommendation,” *ACM TKDD*, vol. 17, no. 1, pp. 1–23, 2023.
- [13] D. Yu, Q. Li, X. Wang, and G. Xu, “Deconfounded recommendation via causal intervention,” *Neurocomputing*, pp. 128–139, 2023.
- [14] X. Du, Z. Wu, F. Feng, X. He, and J. Tang, “Invariant representation learning for multimedia recommendation,” in *MM*, 2022, pp. 619–628.
- [15] Z. Li, D. Amagata, Y. Zhang, T. Hara, S. Haruta, K. Yonekawa, and M. Kurokawa, “Debiasing graph transfer learning via item semantic clustering for cross-domain recommendations,” in *BigData*, 2022, pp. 762–769.
- [16] J. Cao, J. Sheng, X. Cong, T. Liu, and B. Wang, “Cross-domain recommendation to cold-start users via variational information bottleneck,” in *ICDE*, 2022, pp. 2209–2223.
- [17] Z. Wang, S. Shen, Z. Wang, B. Chen, X. Chen, and J.-R. Wen, “Unbiased sequential recommendation with latent confounders,” in *WWW*, 2022, pp. 2195–2204.
- [18] S. Xu, J. Tan, S. Heinecke, V. J. Li, and Y. Zhang, “Deconfounded causal collaborative filtering,” *ACM TORS*, vol. 1, no. 4, pp. 1–25, 2023.
- [19] R. Zhan, C. Pei, Q. Su, J. Wen, X. Wang, G. Mu, D. Zheng, P. Jiang, and K. Gai, “Deconfounding duration bias in watch-time prediction for video recommendation,” in *KDD*, 2022, pp. 4472–4481.
- [20] F. Zhu, Y. Wang, C. Chen, J. Zhou, L. Li, and G. Liu, “Cross-domain recommendation: Challenges, progress, and prospects,” in *IJCAI*, 2021, pp. 4721–4728.
- [21] H. Kanagawa, H. Kobayashi, N. Shimizu, Y. Tagami, and T. Suzuki, “Cross-domain recommendation via deep domain adaptation,” in *ECIR*, 2019, pp. 20–29.
- [22] G. Hu, Y. Zhang, and Q. Yang, “Transfer meets hybrid: A synthetic approach for cross-domain collaborative filtering with text,” in *WWW*, 2019, pp. 2822–2829.
- [23] W. Fu, Z. Peng, S. Wang, Y. Xu, and J. Li, “Deeply fusing reviews and contents for cold start users in cross-domain recommendation systems,” in *AAAI*, 2019, pp. 94–101.
- [24] F. Yuan, L. Yao, and B. Benatallah, “DARec: Deep domain adaptation for cross-domain recommendation via transferring rating patterns,” in *IJCAI*, 2019, pp. 4227–4233.
- [25] F. Zhu, Y. Wang, J. Zhou, C. Chen, L. Li, and G. Liu, “A unified framework for cross-domain and cross-system recommendations,” *IEEE TKDE*, vol. 35, no. 2, pp. 1171–1184, 2021.
- [26] X. Guo, S. Li, N. Guo, J. Cao, X. Liu, Q. Ma, R. Gan, and Y. Zhao, “Disentangled representations learning for multi-target cross-domain recommendation,” *ACM TOIS*, vol. 41, no. 4, pp. 1–27, 2023.
- [27] P. Li and A. Tuzhilin, “Dtdcdr: Deep dual transfer cross domain recommendation,” in *WSDM*, 2020, pp. 331–339.
- [28] M. Liu, J. Li, G. Li, and P. Pan, “Cross domain recommendation via bi-directional transfer graph collaborative filtering networks,” in *CIKM*, 2020, pp. 885–894.
- [29] J. Cao, X. Lin, X. Cong, J. Ya, T. Liu, and B. Wang, “DisenCDR: Learning disentangled representations for cross-domain recommendation,” in *SIGIR*, 2022, pp. 267–277.
- [30] R. Zhang, T. Zang, Y. Zhu, C. Wang, K. Wang, and J. Yu, “Disentangled contrastive learning for cross-domain recommendation,” in *DASFAA*, 2023, pp. 163–178.
- [31] P. Wu, H. Li, Y. Deng, W. Hu, Q. Dai, Z. Dong, J. Sun, R. Zhang, and X.-H. Zhou, “On the opportunity of causal learning in recommendation systems: Foundation, estimation, prediction and challenges,” in *IJCAI*, 2022, pp. 5646–5653.
- [32] S. Xu, J. Ji, Y. Li, Y. Ge, J. Tan, and Y. Zhang, “Causal inference for recommendation: Foundations, methods and applications,” *arXiv preprint arXiv:2301.04016*, 2023.
- [33] M. Sato, S. Takemori, J. Singh, and T. Ohkuma, “Unbiased learning for the causal effect of recommendation,” in *RecSys*, 2020, pp. 378–387.
- [34] D. Liu, P. Cheng, H. Zhu, Z. Dong, X. He, W. Pan, and Z. Ming, “Mitigating confounding bias in recommendation via information bottleneck,” in *RecSys*, 2021, pp. 351–360.
- [35] —, “Debiased representation learning in recommendation via information bottleneck,” *ACM TORS*, vol. 1, no. 1, pp. 1–27, 2023.
- [36] Y. Wang, D. Liang, L. Charlin, and D. M. Blei, “Causal inference for recommender systems,” in *RecSys*, 2020, pp. 426–431.
- [37] Q. Zhang, X. Zhang, Y. Liu, H. Wang, M. Gao, J. Zhang, and R. Guo, “Debiasing recommendation by learning identifiable latent confounders,” in *KDD*, 2023, p. 3353–3363.
- [38] C. Zhao, X. Li, M. He, H. Zhao, and J. Fan, “Sequential recommendation via an adaptive cross-domain knowledge decomposition,” in *CIKM*, 2023, pp. 3453–3463.
- [39] W. Xu, Q. Wu, R. Wang, M. Ha, Q. Ma, L. Chen, B. Han, and J. Yan, “Rethinking cross-domain sequential recommendation under open-world assumptions,” in *WWW*, 2024, pp. 3173–3184.
- [40] J. Ma, C. Zhou, P. Cui, H. Yang, and W. Zhu, “Learning disentangled representations for recommendation,” in *NeurIPS*, 2019, pp. 5711–5722.
- [41] Y. Zheng, C. Gao, X. Li, X. He, Y. Li, and D. Jin, “Disentangling user interest and conformity for recommendation with causal embedding,” in *WWW*, 2021, pp. 2980–2991.
- [42] X. Wang, Q. Li, D. Yu, P. Cui, Z. Wang, and G. Xu, “Causal disentanglement for semantics-aware intent learning in recommendation,” *IEEE TKDE*, vol. 35, no. 10, pp. 9836–9849, 2022.
- [43] K. Zhou, Z. Liu, Y. Qiao, T. Xiang, and C. C. Loy, “Domain generalization: A survey,” *IEEE TPAMI*, vol. 45, no. 4, pp. 4396–4415, 2022.
- [44] J. Wang, C. Lan, C. Liu, Y. Ouyang, T. Qin, W. Lu, Y. Chen, W. Zeng, and S. Y. Philip, “Generalizing to unseen domains: A survey on domain generalization,” *IEEE TKDE*, vol. 35, no. 8, pp. 8052–8072, 2022.
- [45] P. Sheth, R. Moraffah, K. S. Candan, A. Raglin, and H. Liu, “Domain generalization—a causal perspective,” *arXiv preprint arXiv:2209.15177*, 2022.
- [46] S. Zhang, X. Feng, W. Fan, W. Fang, F. Feng, W. Ji, S. Li, L. Wang, S. Zhao, Z. Zhao *et al.*, “Video-audio domain generalization via confounder disentanglement,” in *AAAI*, 2023, pp. 15 322–15 330.
- [47] Y. Liu, Y. Chen, W. Dai, C. Li, J. Zou, and H. Xiong, “Causal intervention for generalizable face anti-spoofing,” in *ICME*, 2022, pp. 01–06.
- [48] Y.-F. Zhang, Z. Zhang, D. Li, Z. Jia, L. Wang, and T. Tan, “Learning domain invariant representations for generalizable person re-identification,” *IEEE TIP*, vol. 32, pp. 509–523, 2022.

- [49] C. Ouyang, C. Chen, S. Li, Z. Li, C. Qin, W. Bai, and D. Rueckert, "Causality-inspired single-source domain generalization for medical image segmentation," *IEEE TMI*, vol. 42, no. 4, pp. 1095–1106, 2022.
- [50] J. Wang, Y. Jiang, Y. Long, X. Sun, M. Pagnucco, and Y. Song, "Deconfounding causal inference for zero-shot action recognition," *IEEE TMM*, vol. 26, pp. 3976–3986, 2023.
- [51] J. Yuan, X. Ma, R. Xiong, M. Gong, X. Liu, F. Wu, L. Lin, and K. Kuang, "Instrumental variable-driven domain generalization with unobserved confounders," *ACM TKDD*, vol. 17, no. 8, pp. 1–21, 2023.
- [52] X. Jin, N. Li, W. Kong, J. Tang, and B. Yang, "Unbiased semantic representation learning based on causal disentanglement for domain generalization," *ACM TOMM*, vol. 20, no. 8, pp. 1551–6857, 2024.
- [53] J. Zhu, Y. Wang, F. Zhu, and Z. Sun, "Domain disentanglement with interpolative data augmentation for dual-target cross-domain recommendation," in *RecSys*, 2023, pp. 515–527.
- [54] P. Ding, Y. Wang, G. Liu, and N. Wang, "Few-shot causal representation learning for out-of-distribution generalization on heterogeneous graphs," *arXiv preprint arXiv:2401.03597*, 2024.
- [55] B. Schölkopf, D. W. Hogg, D. Wang, D. Foreman-Mackey, D. Janzing, C.-J. Simon-Gabriel, and J. Peters, "Modeling confounding by half-sibling regression," *PNAS*, vol. 113, no. 27, pp. 7391–7398, 2016.
- [56] J. Devlin, M. Chang, K. Lee, and K. Toutanova, "BERT: pre-training of deep bidirectional transformers for language understanding," in *NAACL-HLT*, 2019, pp. 4171–4186.
- [57] J.-Y. Zhu, T. Park, P. Isola, and A. A. Efros, "Unpaired image-to-image translation using cycle-consistent adversarial networks," in *ICCV*, 2017, pp. 2223–2232.
- [58] H. Su, J. Li, Z. Du, L. Zhu, K. Lu, and H. T. Shen, "Cross-domain recommendation via dual adversarial adaptation," *ACM TOIS*, vol. 42, no. 3, pp. 1–26, 2023.
- [59] I. Goodfellow, J. Pouget-Abadie, M. Mirza, B. Xu, D. Warde-Farley, S. Ozair, A. Courville, and Y. Bengio, "Generative adversarial nets," *NeurIPS*, 2014.
- [60] Y. Zhu, X. Ren, J. Yi, and Z. Chen, "Deep deconfounded content-based tag recommendation for UGC with causal intervention," *arXiv preprint arXiv:2205.14380*, 2022.
- [61] J. Pearl and D. Mackenzie, *The Book of Why: The New Science of Cause and Effect*. Basic books, 2018.
- [62] X. He, L. Liao, H. Zhang, L. Nie, X. Hu, and T.-S. Chua, "Neural collaborative filtering," in *WWW*, 2017, pp. 173–182.
- [63] C. Zhao, H. Zhao, X. Li, M. He, J. Wang, and J. Fan, "Cross-domain recommendation via progressive structural alignment," *IEEE TKDE*, vol. 36, no. 6, pp. 2401–2415, 2023.
- [64] T. He, K. Li, S. Chen, H. Wang, Q. Liu, X. Wang, and D. Wang, "DMBIN: A dual multi-behavior interest network for click-through rate prediction via contrastive learning," in *SIGIR*, 2023, pp. 1366–1375.
- [65] F. Zhu, Y. Wang, C. Chen, G. Liu, and X. Zheng, "A graphical and attentional framework for dual-target cross-domain recommendation," in *IJCAI*, 2020, pp. 3001–3008.
- [66] D. P. Kingma and J. Ba, "Adam: A method for stochastic optimization," in *ICLR*, 2015.
- [67] X. Wang, X. He, M. Wang, F. Feng, and T.-S. Chua, "Neural graph collaborative filtering," in *SIGIR*, 2019, pp. 165–174.
- [68] X. He, K. Deng, X. Wang, Y. Li, Y. Zhang, and M. Wang, "LightGCN: Simplifying and powering graph convolution network for recommendation," in *SIGIR*, 2020, pp. 639–648.
- [69] T. Man, H. Shen, X. Jin, and X. Cheng, "Cross-domain recommendation: An embedding and mapping approach," in *IJCAI*, 2017, pp. 2464–2470.
- [70] F. Zhu, Y. Wang, C. Chen, G. Liu, M. Orgun, and J. Wu, "A deep framework for cross-domain and cross-system recommendations," in *IJCAI*, 2018, pp. 3711–3717.
- [71] F. Li, H. Liu, J. He, and X. Du, "Causalcdr: Causal embedding learning for cross-domain recommendation," in *SDM*, 2024, pp. 553–561.
- [72] J. Liu, L. Sun, W. Nie, P. Jing, and Y. Su, "Graph disentangled contrastive learning with personalized transfer for cross-domain recommendation," in *AAAI*, 2024, pp. 8769–8777.
- [73] J. Du, Z. Ye, B. Guo, Z. Yu, and L. Yao, "Joint identifiability of cross-domain recommendation via hierarchical subspace disentanglement," *arXiv preprint arXiv:2404.04481*, 2024.
- [74] Z. Lin, H. Ding, N. T. Hoang, B. Kveton, A. Deoras, and H. Wang, "Pre-trained recommender systems: A causal debiasing perspective," in *WSDM*, 2024, pp. 424–433.
- [75] S. Zhang, Q. Miao, P. Nie, M. Li, Z. Chen, F. Feng, K. Kuang, and F. Wu, "Transferring causal mechanism over meta-representations for target-unknown cross-domain recommendation," *ACM TOIS*, vol. 42, no. 4, pp. 1–27, 2024.
- [76] Y. Wang, H. Guo, B. Chen, W. Liu, Z. Liu, Q. Zhang, Z. He, H. Zheng, W. Yao, M. Zhang *et al.*, "Causalint: Causal inspired intervention for multi-scenario recommendation," in *KDD*, 2022, pp. 4090–4099.
- [77] K. Menglin, J. Wang, Y. Pan, H. Zhang, and M. Hou, "C²dr: Robust cross-domain recommendation based on causal disentanglement," in *WSDM*, 2024, pp. 341–349.